Journal of Building Engineering 49 (2022) 104052

Contents lists available at ScienceDirect

Journal of Building Engineering

journal homepage: www.elsevier.com/locate/jobe

Comparison of thermal performance of steel moment and eccentrically braced frames

Seyed Javad Mortazavi [a], Iman Mansouri [b], Paul O. Awoyera [c], Jong Wan Hu [a,d,*]

[a] Department of Civil and Environmental Engineering, Incheon National University, Incheon, 22012, South Korea
[b] Department of Civil and Environmental Engineering, Princeton University Princeton, Princeton, NJ 08544, United States
[c] Department of Civil Engineering, Covenant University, Ota, Nigeria
[d] Incheon Disaster Prevention Research Center, Incheon National University, Incheon, 22012, South Korea

ARTICLE INFO

Keywords:
Fire
Eccentrically braced frame
Moment frame
Finite element
Temperature

ABSTRACT

Eccentrically braced frames (EBFs) are typically employed in seismic design because they integrate the benefits of concentrically braced frames and moment-resisting frames, providing both high elastic stiffness and high ductility. However, the effect of fire on the structural stability of EBFs has not been well documented. Object-oriented techniques used in software program development have become popular in recent years, primarily because of their ability in addressing various complexity issues. Software developed based on an object-oriented approach is more robust than conventional software. Using the abovementioned approach, additional codes can be incorporated, thereby simplifying testing, refining, maintenance, and software extension. Furthermore, the object-oriented approach can be used for finite element analysis. This paper presents the further development of OpenSees software with the inclusion of other parameters: thermal parallel material, thermal spring element, thermal spring section, as well as beam with hinges and thermal elements subjected to fire loading. In contrast to the routine creation of fire-specific applications, these modifications improve the existing finite-element codes, thereby facilitating multi-hazard analysis (e.g., post-earthquake fire). OpenSees is considered in this study as it is an open-source application and suitable for object-oriented design. The abovementioned elements, particularly spring elements, are used extensively in structural simulations (e.g., the modeling of a link beam in an EBF); however, owing to the lack of thermal functions for these elements in OpenSees, the thermal performance of structures that involve these elements cannot be evaluated. Herein, the aforementioned new elements are introduced for the first time; furthermore, the behavior of an EBF system is investigated under thermal loads using open-source software. The thermal performance of EBFs subjected to realistic fire is evaluated in this study based on an analytical modeling of a three-story building. Finally, several compartment fire scenarios are simulated for both EBFs and gravity framing bays. Results show that the EBFs improve the fire performance of the system by extending the time to collapse.

1. Introduction

In the last few decades, the thermal analysis of structures subjected to severe hazards has been performed continually [1–15]. The complete collapse of steel buildings that are subjected to elevated temperatures is rarely considered, although a solution to such a

* Corresponding author. Department of Civil and Environmental Engineering, Incheon National University, Incheon, 22012, South Korea.
E-mail address: jongp24@inu.ac.kr (J.W. Hu).

https://doi.org/10.1016/j.jobe.2022.104052
Received 3 October 2021; Received in revised form 10 January 2022; Accepted 11 January 2022
Available online 14 January 2022

problem would prevent future occurrences of the problem. The complexity of the collapse test, in addition to the cost of performing experiments, is the main constraint in the evaluation of collapse. Meanwhile, structural response during severe hazards can be easily quantified by performing the appropriate numerical simulations. Hence, advanced numerical simulations can facilitate the understanding and quantification of the fire resistance performance of a system, thereby affording an economical and safe structural design.

Strength and stiffness losses are the resulting effects of elevated temperatures on steel structures. In the past two decades, the European steel industry has persistently supported research efforts involving fire-affected steel structures, with the primary aim of promoting the high competitiveness of the material by reducing the cost of passive fire protection applications. Hence, numerous design methods that can be incorporated into the European standards and guidebooks of the steel industry were devised. In the United States, fire protection in steel buildings is achieved through prescriptive considerations [16]. The latter requires both passive and active fire protection measures, as indicated in the International Building Code (IBC) [17]. In active fire protection, sprinkler systems are utilized, whereas in passive fire protection, coating materials are applied to structural elements after the construction of a structure. Depending on the building size or category, the 2018 IBC recommends fulfilling the hourly rating of applied passive fire protection. ASTM E119 [18] and ISO 834 [19] are used to predict the passive protection quantity. Most traditional steel buildings use prescriptive methods, and they can only be justified as effective if they provide the minimum fire resistance threshold. In such cases, the capacity of a member is associated with the limiting temperature. This approach is disadvantageous as it cannot adapt to natural fire cases and the associated uncertainties. Moreover, testing a member in isolation is insufficient, as the structural interaction of components cannot be captured when an entire structure is exposed to fire.

To date, the effect of bracing provisions on the improvement in the disproportionate collapse resistance of steel structures during a fire has not been reported. It was discovered that using hat trusses on a frame top under fire ([9]) can only assist fire load redistribution to columns, i.e., lateral drifts in the column are not resisted; as such, the column is prone to a global downward collapse. Typically, local failure to an entire structure can be prevented by incorporating a vertical bracing system. Therefore, a combined bracing system is preferable for practical applications. Meanwhile, existing studies are primarily associated with two-dimensional (2D) models; hence, its validity and generalization to three-dimensional (3D) buildings is ambiguous. In the current study, the disproportionate collapse of 3D steel-framed structures with bracings subjected to elevated temperatures was investigated. In simulations pertaining to structural fire, three fundamental procedures are considered: the selection of the appropriate design fire, derivation of temperatures for structural members based on design data, and post-fire evaluation of the structure with respect to the derived temperatures. A heat transfer analysis can be performed using well-known structural packages such as ABAQUS, ADINA, ANSYS, F Vulcan, SAFIR, AHTS, and other advanced finite element analysis tools. However, most commercial programs are not affordable; therefore, open-source packages are preferred. Because open-source programs are freely and constantly modified by users, their efficiency is continually improved. OpenSees is an open-source application that has been used widely in recent years. It is an object-oriented program developed by the University of California, Berkeley, and backed by NEES and PEER. OpenSees provides an advanced FE computational process for applications involving the nonlinear structural response of systems under the effects of seismic excitations and fire engineering [20]. Object-oriented programs, unlike algorithm-based programs, enable object interactions their attributes, as well as methods to be viewed.

In this study, an extension is proposed to OpenSees to accommodate thermomechanical analysis in 2D models. The extension involves creating a new pattern of thermal loading, incorporating temperature-dependent properties in the existing material classes, and modifying elements and sections in OpenSees. The system first provides a thermomechanical analysis of structures prior to the hierarchy and architecture description in OpenSees.

By contrast, steel-braced frames are structural systems that are widely utilized for mitigating lateral load demands such as winds and earthquakes [11]. Several types of bracing systems can be employed in the construction of steel buildings. This study focused on eccentrically braced frames (EBFs). In these frames, the braces are designed such that their elasticity is retained during lateral loading. Energy dissipation in these frames occurs by concentrating inelastic deformations in specific regions known as “link beams.” Although steel structures are generally known to perform adequately under elevated temperatures, their performances under such loading conditions are yet to be elucidated. This may have contributed to the considerable deterioration in the strength and stiffness of steel at high temperatures. Hence, specific tests must be performed to simulate the capabilities of steel. From a simulation perspective, the problem is multifaceted and requires the simulation of 1) fire behavior, 2) heat transfer to the structure and among the structural components, and 3) structural response where substantial deformations are expected [13]. For structural engineers, the primary concern is the degradation in the strength and stiffness of steel at high temperatures and the consequential possibility of localized structural failures, which may result in a global system collapse [8,21].

Progressive collapse is a complicated dynamic process, in which a collapsing system searches for other load paths to resist failure in its critical structural members [4]. In this regard, a comprehensive understanding of the response of systems to fire-induced progressive collapse may facilitate the development of performance-based design provisions. Consequently, an economical and safe design of steel structures under fire loading can be developed. Despite numerous studies conducted regarding the seismic behavior of these structures, their behavior under fire loading is yet to be fully investigated.

This main objectives of this study are twofold: (i) to develop of a numerical procedure for determining the fire loading resistance of steel members; (ii) to evaluate the necessity of using components such as brace frames, gravity frames, and moment frames in different fire scenarios.

2. Finite element analysis

In this study, the OpenSees program was further developed to analyze the structural behavior during a fire. In the program, the

structural, fire, and heat transfer models were modified, which rendered OpenSees a fully automated and complete software framework. The OpenSees program analyzes the mechanical behavior of structures under conditions involving a predefined temperature distribution in the structure; in other words, heat transfer and fire models are lacking. Therefore, the latest improvements entail the modification of existing materials, element class (temperature-dependent data), and sections. In addition, a new thermal-load pattern class was created. The authors further developed the OpenSees fire program by performing the following [22]:

- Adding CompositeProtected ENTITIES to model I-shaped steel sections that have a fire-resistive coating material and serve as a composite roof for heat transfer.
- Adding protected HSS ENTITIES to model steel box sections that have a fire-resistive coating material for heat transfer.
- Adding new materials to model fire-resistive coating. The advantage of these materials is that the required coating thickness can be obtained based on a formulation. In addition, they increase the convergence probability of the numerical solution.
- Modifying IsecProtected OpenSees. At the desired cross-section, the coating material was not modeled for the flange thickness; however, we addressed this in our further developed program.
- Defining two new recorder commands to enable temperature information to be extracted from all components of the mesh and elements. Hence, any type of output can be obtained from OpenSees.
- Using the thermal spring element, thermal parallel material, and beam with hinges, which are typically used in the modeling of structural systems.

Several studies [23,24] have reported the development of OpenSees that included static structural analyses under exposure to fire. Convergence methods such as the arch length, Newton, and modified Newton methods are some of the static solutions currently available in OpenSees. The development mentioned above are not essential for progressive collapse analyses, as they can result in a fatal stiffness matrix singularity. Moreover, buckling or failure of structural members may occur because of dynamic loading. Therefore, the progressive collapse of steel frames exposed to fire was analyzed in this study by adopting the existing implicit dynamic operation (Newmark) in OpenSees. A few researchers [25,26] have validated both the procedures pertaining to the structural fire model developed and those of the existing dynamic analysis.

An implicit analysis was adopted as it allows each incremental equation to be solved by performing Newton–Raphson iterations until convergence is attained. All of the above algorithms are deficient for the explicit analysis process, as they do not attain convergence. In a study by Franssen and Gens [27], structures exposed to fire were analyzed based on numerical damping, where the transient nature of fire and dynamic effects were disregarded. In this scenario, they recommended increasing the Newmark parameters β and γ for applications involving the Newmark integrator. It is noteworthy that both the numerical damping rate and stability of the method were affected by the variables. Similar procedures was adopted in the current study. The Newmark integrator was incorporated into OpenSees by setting $\beta = 0.8$ and $\gamma = 0.45$.

In this study, a steel frame beam was subjected to a 14 kN/m uniformly distributed load; UB 305 × 165 × 40 and UC 254 × 254 × 89 universal beams and columns, respectively, were selected. The beam, columns, and bracing were meshed using five elements. All meshed elements were achieved using the *dispBeamColumn-thermal*-type element. The selection of *SteelECThermal* for temperature in steel members was consistent with Eurocode 3. In addition, the ambient temperature yield strength was 356 MPa, and the elastic modulus of the steel was 200 GPa. All the properties of steel were selected in accordance with Eurocode 3 1993 [9] specifications.

The performance of the steel structures exposed to fire loadings was investigated using a three-story EBF, which is consistent with another study [28]. The frame is shown in Fig. 1. The design was executed following the Los Angeles IBC for seismic hazards.

The selected beams and columns are wide flange sections, consistent with ASTM A992, whereas the brace elements were

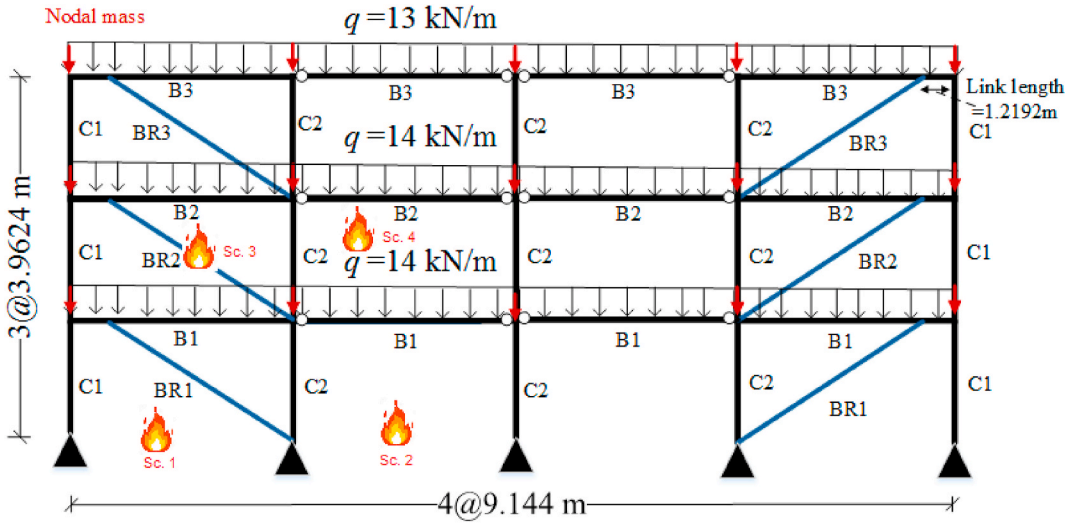

Fig. 1. Layout of three-story EBF.

rectangular HSS sections, consistent with ASTM A500. The open circles in Fig. 1 represent gravity (pinned) connections and were modeled as idealized pins with no rotational stiffness. In addition, the fixed connections were modeled as a fully rigid connection with no failure. However, the connections modeled to demonstrate failure modes can be further investigated in future studies.

To compare the thermal performance of the EBF, a three-story moment frame with the same floor plan and loading was modeled using OpenSees (Fig. 2). This frame was obtained from Ref. [29].

The thermal finite element simulation using OpenSees entails three main stages [20]: stage one involves the prediction of the initial out-of-balance force exerted by the thermal and external loads; stage two involves the use of a stiffness matrix to compute the increase in displacement as a result of the applied force. Finally, stage three involves the conversion of the thermal load to nodal loads using a finite element formulation.

Subsequently, the bays of the structure are modeled. Fig. 1 shows four types of fire scenarios in the bays, denoted as SC1, SC2, SC3, and SC4 for the first, second, third, and fourth floor, respectively. The heating of the beams, columns, and braces occurred in the first bay. Therefore, SC2 and SC4 were for the gravity bays.

The ISO 834 [19] nominal fire curve was used in this study to evaluate fire resistance (Fig. 3); in fact, it has been employed in many studies (e.g., Ref. [30]). The curve shows that an initial temperature increase occurred following an increase in the fire exposure time; hence, the temperature remains constant. However, the decay stage is disregarded because the cooling stage is not considered in the nominal fire curves.

The density of the structural steel was set as 7850 kg/m^3. Generally, the thermal properties of steel are as follows: specific heat, thermal conductivity, coefficient of thermal expansion, and emissivity. Equations (1) and (2) show the expressions for the thermal conductivity as a function of temperature based on Eurocode 3.

$$k = 54 - \left(\frac{T_s}{30}\right) \; for \; 20^{\circ}C < T_s < 800\,^{\circ}C \tag{1}$$

$$k = 27.3 \; for \; T_s \geq 800\,^{\circ}C, \tag{2}$$

where k represents conductivity (W/m°C), and T_s is the steel temperature (°C). Equations (3) and (4) provide the relationship between the specific heat and temperature, as presented in Eurocode 3.

$$C = 425 + 0.773T_s - 0.00169T_s^2 + 2.22 \times 10^{-6}T_s^3 \; for \; 20\,^{\circ}C < T_s < 600\,^{\circ}C \tag{3}$$

$$C = 666 - \frac{13002}{T_s - 738} \; for \; 600\,^{\circ}C < T_s < 735\,^{\circ}C \tag{4}$$

$$C = 545 - \frac{17820}{T_s - 731} \; for \; 735\,^{\circ}C < T_s < 900\,^{\circ}C \tag{5}$$

$$C = 650 \; for \; T_s > 900\,^{\circ}C, \tag{6}$$

where C represents the specific heat (J/kg°C).

It is noteworthy that heat transfer from the fire to the column is primarily caused by the radiation mechanism. Therefore, an

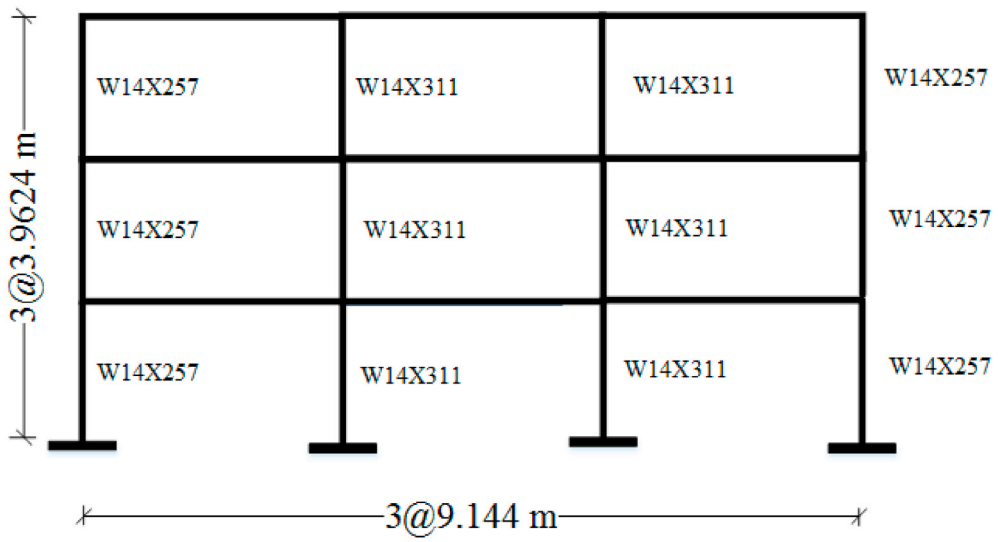

Fig. 2. Layout of three-story moment frame.

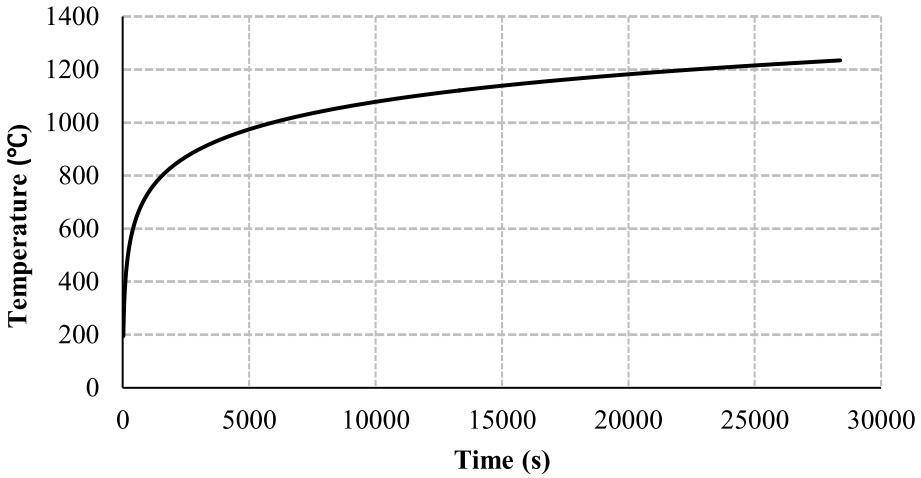

Fig. 3. Actual fire profile (obtained from ISO 834).

accurate estimation of the steel temperatures requires an appropriate steel surface emissivity value. However, some tests may be required to evaluate the emissivity, primarily because surface conditions affect emissivity. In this study, a constant emissivity value of 0.8 was adopted for steel surfaces [31].

In practice, fire protection for steel members is achieved by spraying a fire-resistive substance (FRS). The FRS applied in this study for modeling steel insulation was Blaze Shield (Portland cement-based) applied via spraying at a density of 240 kg/m^3 [32]. Available data pertaining to the specific heat and thermal conductivity of Blaze Shield (up to 1200 °C) in the NIST SP 1000-5(2004) standard were utilized in this study. Table 1 shows the data; as shown, both the thermal conductivity and specific heat increased with temperature.

The FRS of Blaze is known to exhibit lower strength and stiffness than steel; this indicates that it will not significantly affect the structural performance. Hence, the FRS was disregarded in the current analysis. The thickness of the FRS was 45 mm for a 3 h fire loading, which was calculated using Equation (7) [32].

$$h = \frac{R}{1.01\frac{W}{D} + 0.66} \tag{7}$$

where h represents the FRS thickness (which ranges between 0.375 and 3.75 inches), W the steel column weight, R the duration of fire resistance (in hours), and D the heated perimeter of the steel column (in inches). This material is not available in the current version of OpenSees; however, the authors were able to add it to the OpenSees library.

Before executing the main OpenSees file, a heat transfer analysis was conducted for all member sections. By applying a fire profile at any point in the section, the temperature changes over time can be obtained, and these temperatures become the input for the main file of the model. In OpenSees, the FEM was utilized to solve the transient fundamental equations for heat transfer. As such, the mesh tool was used for model discretization. In this regard, the geometry of the section was created using *HTEntity*. The seed distribution for the mesh was generated using the *HTMesh* command. The specific details for each type of structural member are as follows:

i) Columns: The *HTEntity ProtectedIsection* command was used to generate I-shaped sections (Fig. 4). The thickness of the SFRM was calculated using Equation (7), and the perimeter of the I-shaped section was regarded as that of the SFRM. In addition, *HTMaterial CarbonSteelEC3* and *HTMaterial SFRM* were selected as the material properties of steel and the SFRM, respectively, where the latter was developed by the authors and newly added in OpenSees. In addition, in the current version of OpenSees, the SFRM is not

Table 1
Variation in FRS thermal conductivity and specific heat with temperature [32].

Temperature (°C)	Conductivity (W/m°K)	Specific heat (J/kg°K)
20	0.042	797
50	0.072	868
100	0.093	712
200	0.088	924
300	0.106	1086
400	0.134	1149
500	0.169	1252
600	0.216	1293
800	0.275	1369
1000	0.369	1412
1200	0.407	1462

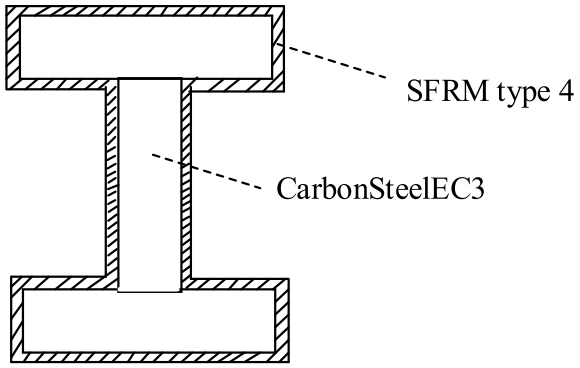

Fig. 4. Steel column section model in OpenSees.

modeled for the flange thickness. However, the authors rectified this issue such that during heat transfer analysis, the SFRM is modeled around the section.

Braces: The authors developed the *HTEntity HSSProtected* command to generate box (HSS) sections (Fig. 5). The thickness of the SFRM was calculated using Equation (7), and the perimeter of the HSS section was regarded as that of the SFRM. In addition, *HTMaterial CarbonSteelEC3* and *HTMaterial SFRM* were selected as the material properties of steel and the SFRM, respectively.

ii) Beams: The *HTEntity CompositeProtected* command was used to generate the I-shaped beam sections (Fig. 6). The thickness of the SFRM was calculated using Equation (7), and the perimeter of the I-shaped section, except for the top flange, was regarded as that of the SFRM. A concrete slab with a thickness of 100 mm was assumed at the top of the beam section. In addition, *HTMaterial CarbonSteelEC3, HTMaterial SFRM*, and *ConcreteEC2* were selected as the material properties of steel, the SFRM, and concrete, respectively.

The heat transfer coefficients at the boundary were defined using the *HTConstants* command, whereas the *HeatFluxBC* command was used to define radiation, convection, or other prescribed heat fluxes. Finally, using a fire profile, heat was applied to all faces of the column and brace sections.

Moreover, *the HTConstants* command was used to define the coefficients for the heat transfer boundary conditions, which were used in association with *the HeatFluxBC* command when defining convection and radiation or prescribed heat fluxes. Finally, using a fire profile, heat was applied to all faces of the column and brace sections. Fig. 7 shows the result of the heat transfer analysis in OpenSees; the thermal contour was plotted after post-processing the result.

It should be noted that the modeling of bond between SFRM and steel at ambient and fire conditions plays an important role in results. However, due to the limitations of modeling in the current version of the software, it is not possible to consider the debonding, which is why in the technical literature [5,33–39], modeling has been done in the same way and with simplification. Besides, this study is related to two-dimensional models in which modeling of the deboding behavior is not easily done. All materials used in structural modeling are subject to temperature changes, in other words, their modulus of elasticity and yield stress are based on the temperature function regulations. As mentioned earlier, some elements in the current version of the software do not include this issue, but the authors have been able to add thermal modules to them.

3. Verification

Verification is important in numerical studies. The capability of the model in predicting the response to fire at the building level was determined by validating the FE model as an entire system as an individual members. Hence, the model-predicted mechanical and thermal-response-measured data were compared via fire tests. The EBF link beams and other beams were validated for beam thermal analysis.

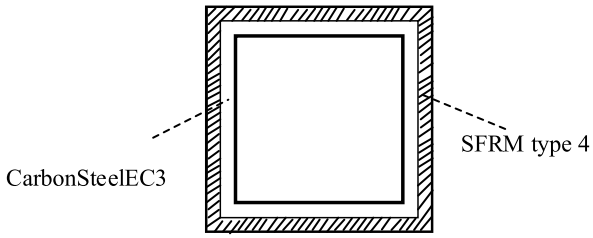

Fig. 5. Steel brace section model in OpenSees.

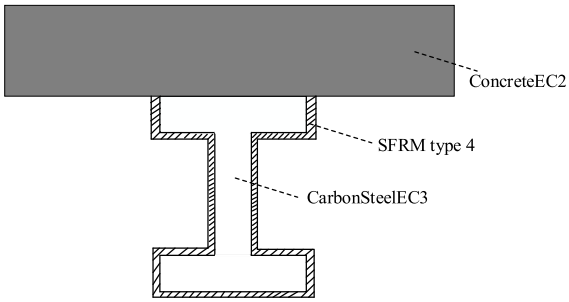

Fig. 6. Steel beam section model in OpenSees.

3.1. EBF link model

A typical OpenSees model of the experimental setup is shown in Fig. 8. Reverse cyclic static loading with varying displacement amplitudes was indicated in both the model and experiment (AISC seismic provisions). In addition, a hysteretic plot correlating force and displacement for the OpenSees model and 4A-RLP experimental data is shown in Fig. 9.

Fig. 9 shows that the result of the OpenSees model is consistent with the experimental result. It is noteworthy that in the case involving links in the EBF, to generate a tri-spring shear material behavior, *uniaxialMaterial Parallel* was used. The current version of the OpenSees fire program does not include the thermal functions of the spring element and *uniaxialMaterial Parallel*. However, the authors successfully developed them [22].

3.2. Thermal analysis

An analysis of a simply supported steel I-shaped beam (1.14 m span IPE80 (ST37) section) was performed in a previous study [42]. In that study, a point load of different load ratios was imposed at the mid-span of the beam, and the temperature profile was increased uniformly. The EBF modeling procedures in OpenSees were replicated for the experimental data models. As shown in Fig. 10, the experimental data agreed well with the OpenSees generated data in terms of the mid-span deflection and temperature.

4. Results and discussion

Herein, to compare the EBF and MRF systems under fire conditions, the behavior of these systems was investigated for the four fire scenarios, as shown in Fig. 1 For each fire scenario, the internal force of the columns and the deformation of the beam corresponding to the bay of the frame in which the scenario was subjected to heat load were extracted. In Fig. 11, which shows the axial force of the left column in different scenarios, scenario 1 depicts the axial force of column C11; scenario 2, the axial force of column C12; scenario 3, the axial force of column C21; and scenario 4, the axial force of column C22. In addition, in Fig. 12, which pertains to the axial force of the column on the right side of the bay under fire, scenarios 1 to 4 are associated with the axial force of columns C12, C22, C21, and C22, respectively. In Fig. 13, the diagrams for Scenarios 1 to 4 show the deformation changes in the middle of beams B11, B12, B21, and B22, respectively (see Figs. 14–19).

4.1. Thermal behavior of MRF

In Scenario 1, the fire load affected the frame members at 650 °C. Prior to that, the SFRM coating prevented an increase in the steel material temperature. After that point, because of the increase in the steel temperature, the stiffness of beam B11 decreased, whereas its axial elongation increased. Owing to the increased axial deformation of beam B11, the top of column C11 inclined to the left, which resulted in the formation of a secondary moment in it (Fig. 11). As the temperature was increased further, the modulus of elasticity of the beam decreased; consequently, whereas the load on the beam was almost constant, the first plastic joint was formed at the junction of the beam to column C12. Immediately after the formation of this plastic joint, a plastic joint was formed at the connection of the beam to column C11. Thereafter, the manner by which the load was transferred in the structure changed because beam B11 served as a two-headed joint beam; consequently, the structure maintained its stability by reproducing the loads entering the beam. In this regard, columns C12 and C11 were predicted to contribute the most significantly (Fig. 12). However, because the columns were exposed to heat (which reduced the modulus of elasticity and consequently the stiffness of the limb), columns C22 and C21 also contributed significantly. As the temperature increased, the modulus of elasticity of iron decreased, resulting in a decrease in the stiffness of the members to which the fire load was applied. This reduction in stiffness reduced the bearing capacity of the C11 column, which was offset by the C21 and B21 beams. As the temperature increased, a third plastic joint was formed in the middle of the B11 beam. Thereafter, B11 beam could not transfer the loads to it; therefore, it underwent extremely large deformations. As the temperature increased further, the C11 and C22 columns buckled, and the structure collapsed. The midpoint deflection of the beam is shown in Fig. 13.

In the second scenario, as the temperature increased, the two ends of the B12 beam formed a plastic joint. Subsequently, a plastic joint was formed in the middle of this beam; finally, as the temperature increased further, buckling occurred in columns C12 and C13, and then the structure collapsed.

In the third scenario, by increasing the temperature in beam B21, the expansion of the beam caused columns C21 and C31 to be

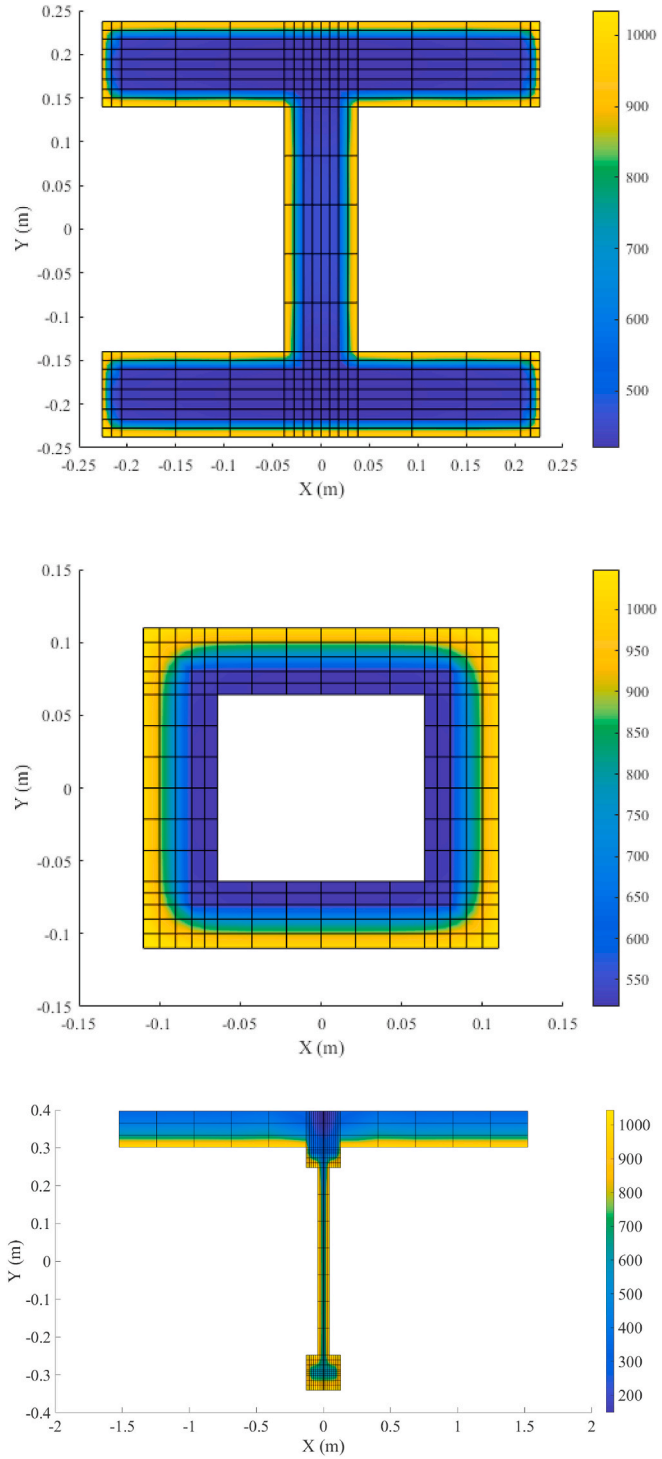

Fig. 7. Heat transfer obtained from OpenSees for (a) column, (b) brace, and (c) beam section.

deformed laterally. This deformation caused beam B11 to deform and increase negatively. As the temperature increased, the first organ to deform the plastic was the B21 beam. Initially, the two ends of the beam were formed by a plastic joint, and after the temperature increased, a plastic joint was formed in the middle of the beam. Thereafter, the beam underwent significant deformations, which reduced the lateral deformation of columns C21 and C31; in fact, this was due to the axial deformation of the beam caused by the expansion of the ax iron. Finally, as the temperature increased, column C22 and a column in its vicinity, i.e., column C21, buckled;

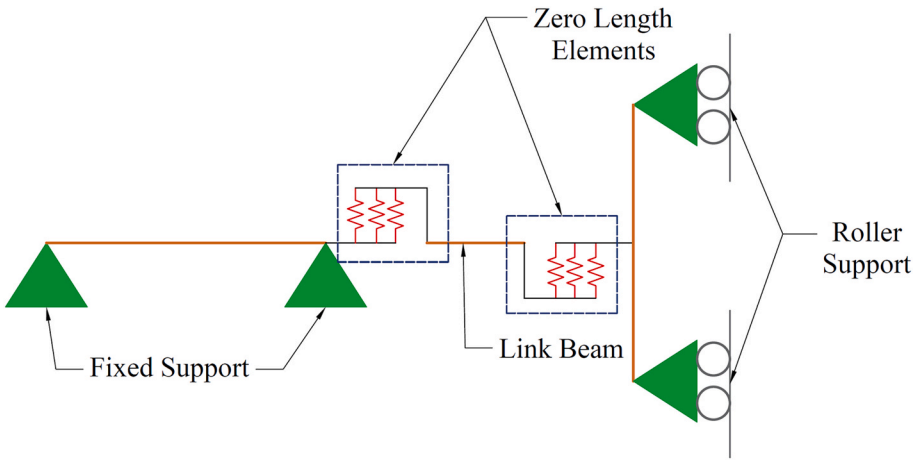

Fig. 8. Simulation of experimental setup using OpenSees model [40].

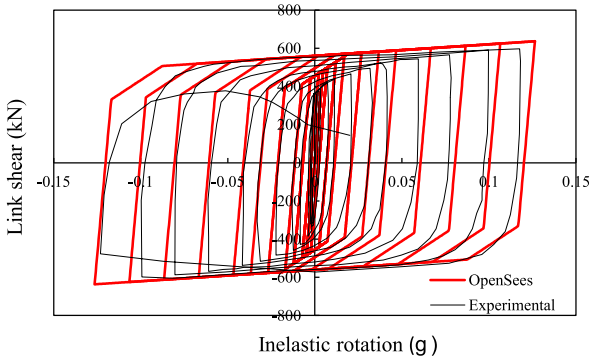

Fig. 9. Hysteretic link behavior based on (a) experiment [41] and (b) OpenSees link model.

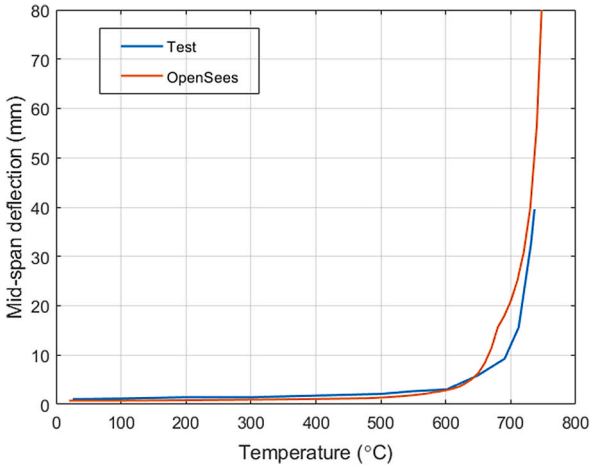

Fig. 10. OpenSees model and experimental data [42] comparison.

consequently, the structure collapsed.

In the fourth scenario, axial deformation due to the expansion of the beam material occurred first in beam B22. As the temperature of the beam increased further, a plastic joint was formed at both ends of the beam, and the force transmission in the structure changed. Subsequently, a plastic joint was formed in the middle of the beam, and the beam exhibited large deformations. Next, the two adjacent columns, namely columns C22 and C23, buckled, and then the structure collapsed.

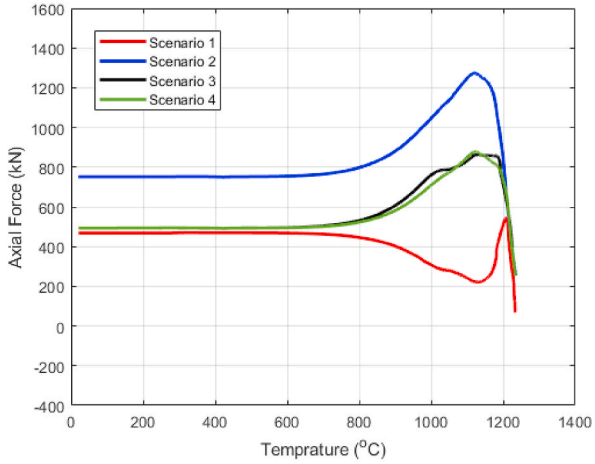

Fig. 11. Left column axial force in different scenarios for MRF.

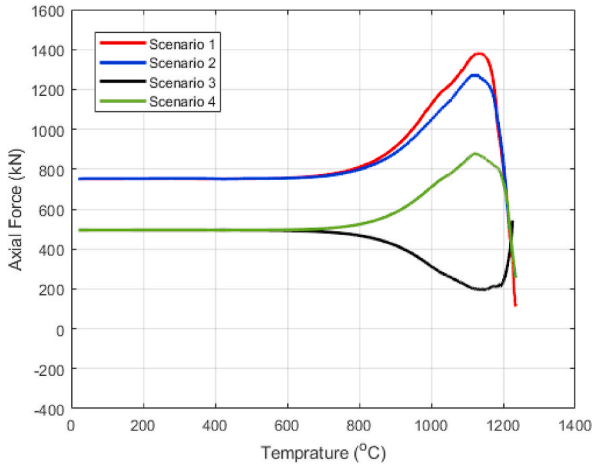

Fig. 12. Right column axial force in different scenarios for MRF.

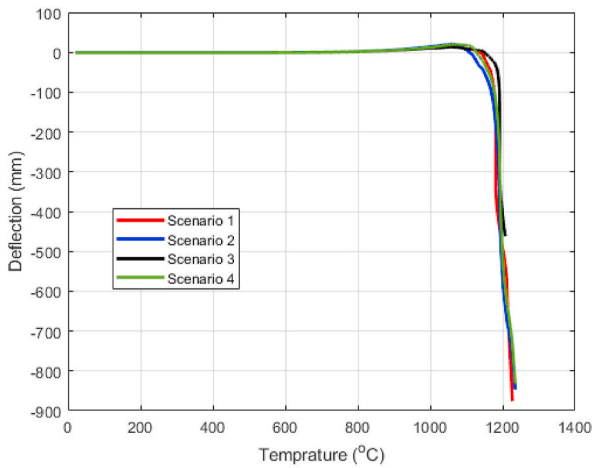

Fig. 13. Beam midpoint deflection in different scenarios for MRF.

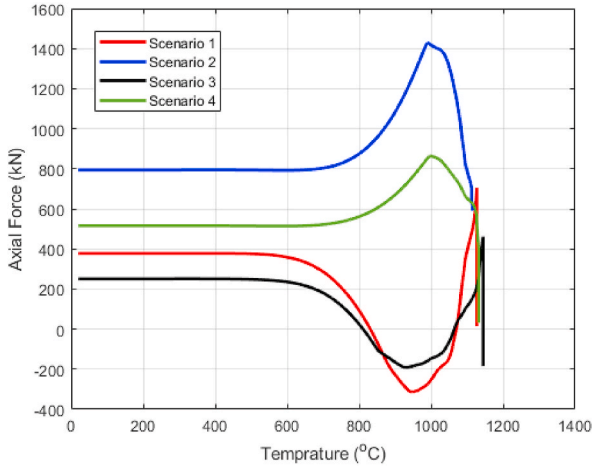

Fig. 14. Left column axial force in different scenarios for EBF.

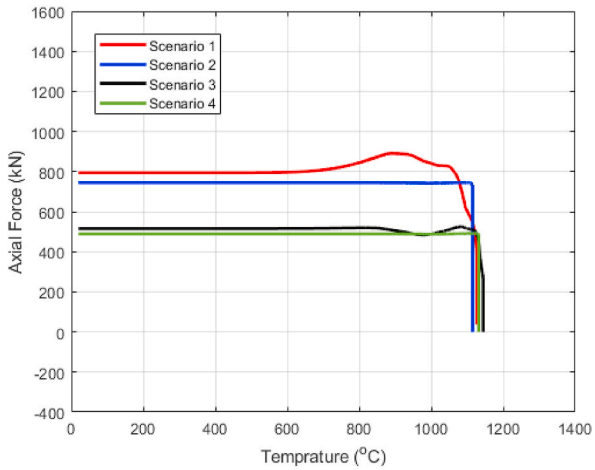

Fig. 15. Right column axial force in different scenarios for EBF.

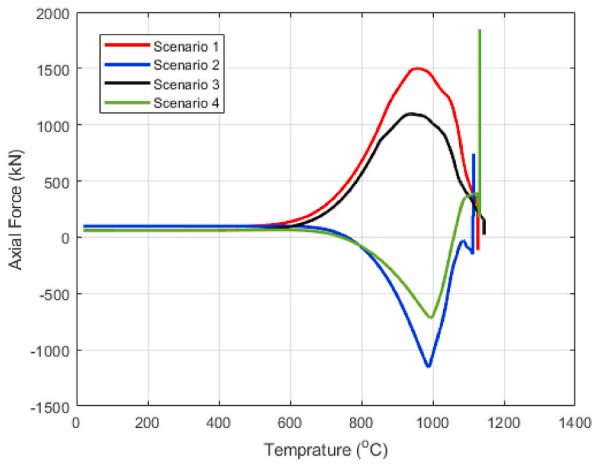

Fig. 16. Brace axial force in different scenarios for EBF.

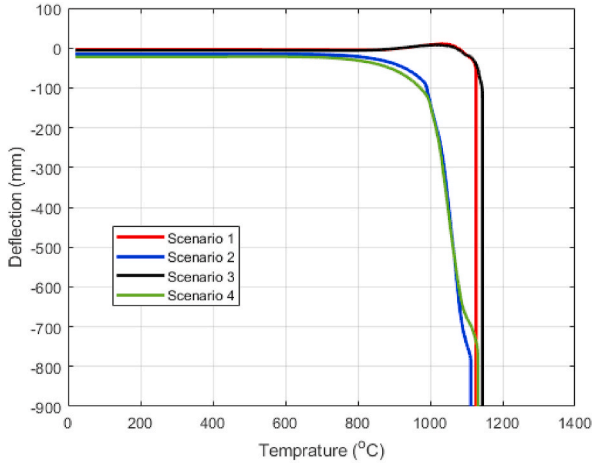

Fig. 17. Beam midpoint deflection in different scenarios for EBF.

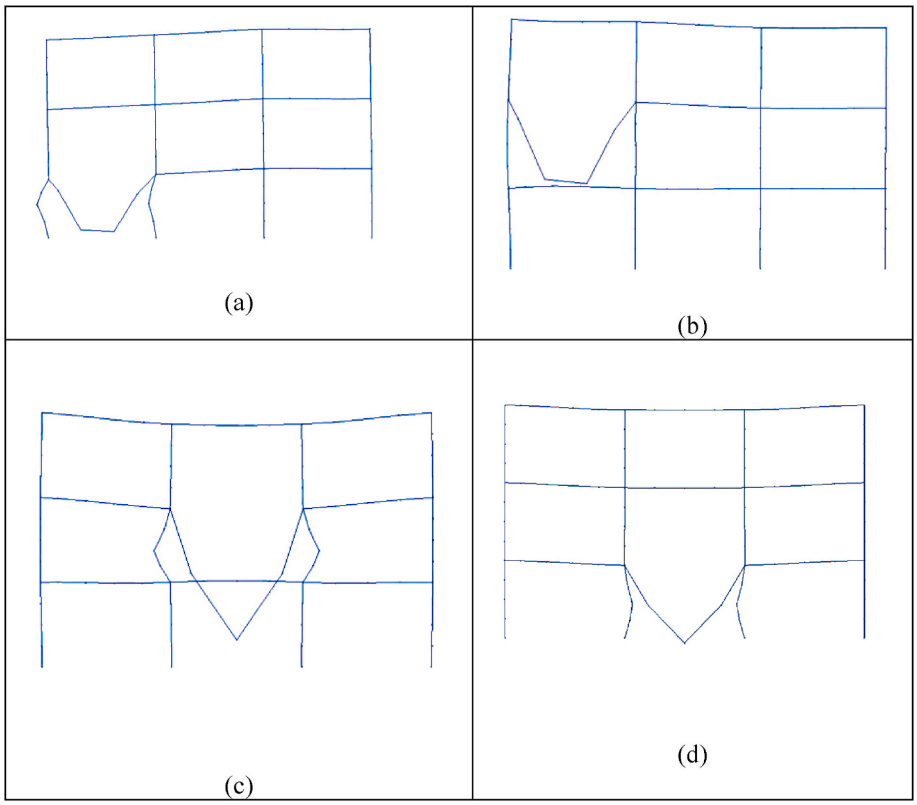

Fig. 18. Deflected shapes of MRF at onset of collapse for fire scenarios (a) 1, (b) 2, (c) 3, and (d) 4.

4.2. Thermal behavior of EBF

In the first scenario, beam B11 deformed in the positive direction up to a temperature of approximately 1080 °C; thereafter, owing to the formation of the plastic joint due to the decrease in the modulus of elasticity, it deformed rapidly and significantly in the direction of plastic deformation. This occurred until the structure collapsed at a temperature of 1120 °C. In the second scenario, beam B12 deformed at approximately 800 °C in the direction of elastic deformation. Thereafter, the deformation continued rapidly in the plastic joint beam until 990 °C, which resulted in an extremely large deformation in the beam; finally, the beam collapsed at a temperature of 1100 °C. Beam B21 in the third scenario under heat behaved similarly to beam B11 in the first scenario. Beam B22 in the fourth scenario, under the heat effect of fire, underwent deformations similar to beam B12 in the second scenario.

Although the imperfection plays an important role in thin members, the results of this study showed that it does not have a

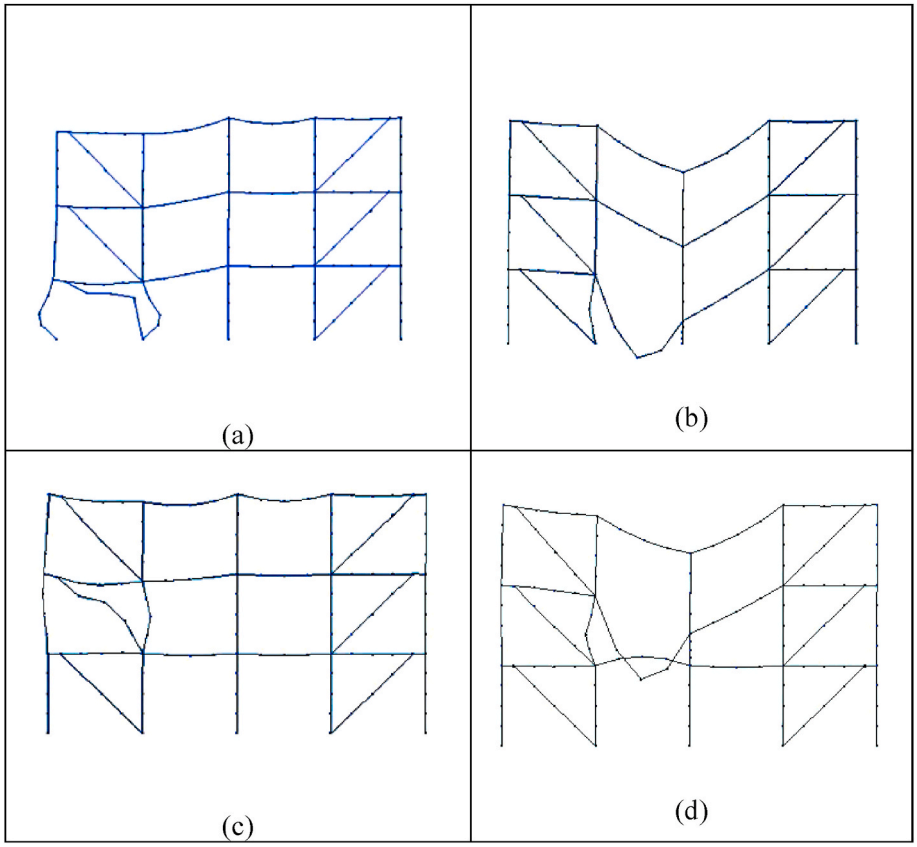

Fig. 19. Deflected shapes of EBF at onset of collapse for fire scenarios (a) 1, (b) 2, (c) 3, and (d) 4.

significant effect. At the same time, in Eurocode regulations, the yield stress versus temperature is less than the actual state to take into account the effects of creep.

5. Conclusions

A modeling approach and validation results for modeling an EBF exposed to elevated temperatures were presented herein. The authors further developed the OpenSees fire program by performing the following: (i) adding CompositeProtected ENTITIES to model I-shaped steel sections that have a fire-resistive coating material and serve as a composite roof for heat transfer, (ii) adding protected HSS ENTITIES to model steel box sections that have a fire-resistive coating material for heat transfer, and (iii) adding a new material to model the fire-resistive coating. The advantage of the material is that the required coating thickness can be obtained based on a formulation. In addition, it increases the probability of convergence in the numerical solution and modification of IsecProtected in OpenSees. At the desired cross-section, the coating material was not modeled for the flange thickness. However, the authors successfully modified it by defining two new recorder commands to enable temperature information to be extracted from all components of the mesh and elements. Consequently, any type of output can be obtained from OpenSees. Furthermore, the thermal spring element, thermal parallel material, and beam with hinges, which are typically used in the modeling of structural systems, were adopted. In a case study, three-story EBF and MRF structures were subjected to four fire scenarios. The corresponding evolution of the progressive collapse was investigated, and the results showed that columns in gravity bays failed sooner than columns in EBF bays. Furthermore, the braces redistributed the load and prolonged the eventual progressive collapse of the bending frame in all the scenarios investigation. First, the beams deformed; subsequently, a plastic joint was formed in them. After the formation of three plastic joints in the beams, the columns buckled, which then caused the structure to collapse. However, in the bracing frames, a different phenomenon occurred. In those frames, the bracing buckled, followed immediately by the columns that were affected by the fire; subsequently, the beams underwent large deformations. In the openings of the bracing frame that did not have a seal, such as in the second and fourth scenarios, owing to the joint connection of the beams, a plastic joint was formed first in the middle of the beam opening. Subsequently, as the temperature increased, the column adjacent to the beam, which was only under an axial load, lost its load owing to the decrease in the modulus of elasticity and resistance due to the increase in temperature. Finally, the structure collapsed.

Author statement

Iman Mansouri: Conceptualization, Project supervision, Writing—Review and Editing. Seyed Javad Mortazavi: Formal analysis, Investigation, Writing—Original Draft preparation Paul Oluwaseun Awoyera: Writing—Review and Editing Jong-Wan Hu: Writing—Review, Editing and Funding acquisition.

Declaration of competing interest

The authors declare that they have no known competing financial interests or personal relationships that could have appeared to influence the work reported in this paper.

Acknowledgments

This study was supported by a National Research Foundation of Korea (NRF) grant funded by the Korean government (MSIT) (NRF-2021R1A2B5B02002599).

References

[1] A. Abu, V. Ramanitrarivo, I. Burgess, Collapse mechanisms of composite slab panels in fire, J. Struct. Fire Eng. 2 (3) (2011) 205–215, https://doi.org/10.1260/2040-2317.2.3.205.
[2] G. Cooke, When are sandwich panels safe in fire? Part 2 - avoiding collapse, Fire Eng. J. 58 (196) (1998) 25–32.
[3] J. Jiang, G.Q. Li, Mitigation of fire-induced progressive collapse of steel framed structures using bracing systems, Adv. Steel Construct. 15 (2) (2019) 192–202, https://doi.org/10.18057/IJASC.2019.15.2.9.
[4] J. Jiang, G.Q. Li, A. Usmani, Effect of bracing systems on fire-induced progressive collapse of steel structures using OpenSees, Fire Technol. 51 (5) (2015) 1249–1273, https://doi.org/10.1007/s10694-014-0451-0.
[5] J. Jiang, Y. Lu, X. Dai, G.Q. Li, W. Chen, J. Ye, Disproportionate collapse of steel-framed gravity buildings under travelling fires, Eng. Struct. 245 (2021), https://doi.org/10.1016/j.engstruct.2021.112799.
[6] G.Q. Li, W. Ji, C.Y. Feng, Y. Wang, G.B. Lou, Experimental and numerical study on collapse modes of single span steel portal frames under fire, Eng. Struct. 245 (2021), https://doi.org/10.1016/j.engstruct.2021.112968.
[7] M.Z. Naser, V. Kodur, H.T. Thai, R. Hawileh, J. Abdalla, V.V. Degtyarev, StructuresNet and FireNet: benchmarking databases and machine learning algorithms in structural and fire engineering domains, J. Build. Eng. 44 (2021), https://doi.org/10.1016/j.jobe.2021.102977.
[8] C. Qin, Collapse Simulations of Steel Buildings under Fire, Master thesis, Colorado State University, 2016.
[9] C. Qin, H. Mahmoud, Collapse performance of composite steel frames under fire, Eng. Struct. 183 (2019) 662–676, https://doi.org/10.1016/j.engstruct.2019.01.032.
[10] R. Chicchi, A. Varma, Assessment of post-earthquake fire behavior of a steel MRF building in a low seismic region, Int. J. Steel Struct. 18 (4) (2018) 1470–1481, https://doi.org/10.1007/s13296-018-0183-y.
[11] J.W. Hu, R. Chicchi, I. Mansouri, S.J. Mortazavi, J.J. Kim, Thermal performance of steel eccentrically braced frames subjected to fire conditions, in: 10th International Symposium on Steel Structures, November 13-16, 2019, Jeju, Korea, 2019, https://doi.org/10.1016/j.jcsr.2021.106691.
[12] R. Solhmirzaei, H. Salehi, V. Kodur, M.Z. Naser, Machine learning framework for predicting failure mode and shear capacity of ultra high performance concrete beams, Eng. Struct. 224 (2020), https://doi.org/10.1016/j.engstruct.2020.111221.
[13] R. Sun, Z. Huang, I.W. Burgess, Progressive collapse analysis of steel structures under fire conditions, Eng. Struct. 34 (2012) 400–413, https://doi.org/10.1016/j.engstruct.2011.10.009.
[14] Y. Wang, V.K.R. Kodur, C. Fu, C. Liu, H. Zhou, M.Z. Naser, Seismic performance of reinforced concrete frame joints after exposure to fire, ACI Struct. J. 118 (3) (2021) 3–14, https://doi.org/10.14359/51731586.
[15] Y. Zhou, J. Yang, Z. Wang, H.J. Hwang, Y. Huang, L. Deng, W. Yi, Static load test on the progressive collapse resistance of precast concrete frame substructure during and after high temperature, J. Struct. Eng. 147 (8) (2021), https://doi.org/10.1061/(ASCE)ST.1943-541X.0003072.
[16] M.M. Drury, Numerical Investigation of Composite Floor Beam Resilience to Realistic Fire Scenarios, Master Thesis, Lehigh University, 2019.
[17] International Code Council (ICC), International Building Code, 2014.
[18] ASTM Standard E119-18, Standard Test Methods for Fire Tests of Building Construction and Materials, 2018.
[19] International Organization for Standardization, ISO 834-13, 2019.
[20] N. Elhami Khorasani, M.E.M. Garlock, S.E. Quiel, Modeling steel structures in OpenSees: enhancements for fire and multi-hazard probabilistic analyses, Comput. Struct. 157 (2015) 218–231, https://doi.org/10.1016/j.compstruc.2015.05.025.
[21] E. Talebi, M. Md Tahir, F. Zahmatkesh, A.B.H. Kueh, Comparative study on the behaviour of buckling restrained braced frames at fire, J. Constr. Steel Res. 102 (2014) 1–12, https://doi.org/10.1016/j.jcsr.2014.06.003.
[22] S.J. Mortazavi, I. Mansouri, P.O. Awoyera, M.Z. Naser, Implementation of new elements and material models in OpenSees software to account for post-earthquacke fire damage, Structures 27 (2020) 1777–1785, https://doi.org/10.1016/j.istruc.2020.08.021.
[23] J. J, Nonlinear Thermomechanical Analysis of Structures Using OpenSees, Ph.D., University of Edinburgh, England, 2012.
[24] J. Jiang, L. Jiang, P. Kotsovinos, J. Zhang, A. Usmani, F. McKenna, G.Q. Li, OpenSees software architecture for the analysis of structures in fire, J. Comput. Civ. Eng. 29 (1) (2015), https://doi.org/10.1061/(ASCE)CP.1943-5487.0000305.
[25] J. Jiang, G.Q. Li, A. Usmani, Progressive collapse mechanisms of steel frames exposed to fire, Adv. Struct. Eng. 17 (3) (2014) 381–398, https://doi.org/10.1260/1369-4332.17.3.381.
[26] J. Jiang, A. Usmani, G.Q. Li, Modelling of steel-concrete composite structures in fire using OpenSees, Adv. Struct. Eng. 17 (2) (2014) 249–264, https://doi.org/10.1260/1369-4332.17.2.249.
[27] J.M. Franssen, F. Gens, Dynamic Analysis Used to Cope with Partial and Temporary Failures, Third International Workshop - Structures in Fire, 2004, pp. 297–310.
[28] S.H. Chao, S.C. Goel, Performance-based Seismic Design of EBF Using Target Drift and Yield Mechanism as Performance Criteria, Report No. UMCEE 05-05, Department of Civil and Environmental Engineering, The University of Michigan, Ann Arbor, MI, 2005.
[29] A. Gupta, H. Krawinkler, Seismic Demands for Performance Evaluation of Steel Moment Resisting Frame Structures, 1999. John A Blume Earthquake Engineering Center Technical Report 132. Stanford Digital Repository, http://purl.stanford.edu/fm826wn5553.
[30] Y.E. Akbulut, A.C. Altunişik, H.B. Başağa, S. Mostofi, A. Mosallam, L.F. Wafa, Elevated temperature effect on the dynamic characteristics of steel columns and frames, Int. J. Steel Struct. 21 (3) (2021) 861–882, https://doi.org/10.1007/s13296-021-00479-w.
[31] T.R. Kay, B.R. Kirby, R.R. Preston, Calculation of the heating rate of an unprotected steel member in a standard fire resistance test, Fire Saf. J. 26 (4) (1996) 327–350, https://doi.org/10.1016/S0379-7112(96)00016-1.
[32] Y.K. Kwak, S. Pessiki, K. Kwon, Fire behavior of steel columns encased by damaged spray-applied fire resistive material, Archit. Res. 10 (1) (2008) 1–11.
[33] Q. Guo, A.E. Jeffers, Finite-element reliability analysis of structures subjected to fire, J. Struct. Eng. 141 (4) (2015), https://doi.org/10.1061/(ASCE)ST.1943-541X.0001082.

[34] M. Dwaikat, V. Kodur, Modeling fracture and delamination of spray-applied fire-resisting materials under static and impact loads, J. Eng. Mech. 137 (12) (2012) 901–910, https://doi.org/10.1061/(ASCE)EM.1943-7889.0000290.
[35] S.E. Quiel, S.M. Marjanishvili, Fire resistance of a damaged steel building frame designed to resist progressive collapse, J. Perform. Constr. Facil. 26 (4) (2012) 402–409, https://doi.org/10.1061/(ASCE)CF.1943-5509.0000248.
[36] C. Zhang, A. Pintar, J.M. Weigand, J.A. Main, F. Sadek, Impact of variability in thermal properties of SFRM on steel temperatures in fire, Fire Saf. J. 123 (2021) 103361, https://doi.org/10.1016/j.firesaf.2021.103361.
[37] I.-R. Choi, High-temperature thermal properties of sprayed and infill-type fire-resistant materials used in steel-tube columns, Int. J. Steel Struct. 20 (3) (2020) 777–787, https://doi.org/10.1007/s13296-020-00322-8.
[38] S. Venkatachari, V.K.R. Kodur, System level response of braced frame structures under fire exposure scenarios, J. Constr. Steel Res. 170 (2020) 106073, https://doi.org/10.1016/j.jcsr.2020.106073.
[39] J. Martinez, A.E. Jeffers, Structural response of steel-concrete composite floor systems under traveling fires, J. Constr. Steel Res. 186 (2021) 106926, https://doi.org/10.1016/j.jcsr.2021.106926.
[40] G. Prinz, Using Buckling-Restrained Braces in Eccentric Configurations, Ph.D. thesis, Brigham Young University, USA, 2010.
[41] T. Okazaki, G. Arce, H.C. Ryu, M.D. Engelhardt, Experimental study of local buckling, overstrength, and fracture of links in eccentrically braced frames, J. Struct. Eng. 131 (10) (2005) 1526–1535, https://doi.org/10.1061/(ASCE)0733-9445(2005)131:10(1526).
[42] A. Rubert, P. Schaumann, Structural steel and plane frame assemblies under fire action, Fire Saf. J. 10 (3) (1986) 173–184, https://doi.org/10.1016/0379-7112(86)90014-7.